RESEARCH ARTICLES

Scheme construction with numerical flux residual correction (NFRC) and group velocity control (GVC)*

MA Yanwen** and FU Dexun

(LNM, Institute of Mechanics, Chinese Academy of Sciences, Beijing 100080, China)

Received February 27, 2006; revised June 9, 2006

Abstract For simulating multi-scale complex flow fields like turbulent flows, the high order accurate schemes are preferred. In this paper, a scheme construction with numerical flux residual correction (NFRC) is presented. Any order accurate difference approximation can be obtained with the NFRC. To improve the resolution of the shock, the constructed schemes are modified with group velocity control (GVC) and weighted group velocity control (WGVC). The method of scheme construction is simple, and it is used to solve practical problems.

Keywords: high order accurate scheme, group velocity control, high resolution of the shock.

To simulate the multi-scale complex flow fields, like turbulence, high order accurate schemes are preferred. There are many ways to construct high order accurate schemes[1,2], but most of them are complicated, and a system of linear algebraic equations has to be solved. In 1992, we constructed the fourth order symmetrical compact difference approximation by using residual correction from lower order difference approximation[3]. In 2001 and 2002, Lerat and Corre constructed a traditional fourth order accurate approximation with residual correction from the second order accurate difference approximation[4,5]. These scheme constructions are simple, but the schemes were constructed only for the particular cases. In this paper we present a simple method for construction of the high order accurate schemes using numerical flux residual correction, and the scheme construction with numerical flux residual correction for more general cases is presented.

When high order accurate schemes are used to solve problems with discontinuities, the oscillations will be produced in the numerical solutions. To improve the resolution of the shock, many good schemes with high resolution of the shocks have to be developed, and many practical problems have been solved with these schemes[6—12]. As is known, the total variation diminishing (TVD) scheme can capture the shocks well[6], but the accuracy of the schemes is too low to simulate the complex flows with a wide range of scales. The dissipation of the scheme is large, and the accuracy of the schemes will be reduced at the extreme points. Essentially non-oscillatory (ENO) and weighted essentially non-oscillatory (WENO) schemes have high order accuracy, but they are complicated and computer time consuming[7—10]. WENO scheme was greatly improved in Refs. [9—11]. In Ref. [12], the behavior of the numerical solutions is analyzed and GVC is used to improve the resolution of discontinuities.

In this paper, a class of schemes constructed with NFRC is presented. To improve the resolution of the shock, the constructed schemes are modified with GVC and WGVC.

1 Numerical flux residual correction (NFRC)

Consider a model equation and its semi-discrete approximation

$$\frac{\partial u}{\partial t}+\frac{\partial f}{\partial x}=0, \quad f=cu, \quad c=\text{const}, \tag{1}$$

$$\frac{\partial u_j}{\partial t}+\frac{F_j}{\Delta x}=0. \tag{2}$$

Define

$$\Delta x\left(\frac{\partial f}{\partial x}\right)_j=F_j, \quad F_j=h_{j+1/2}-h_{j-1/2},$$

where $h_{j+1/2}$ is the numerical flux. For the first order

* Supported by the National Natural Science Foundation of China (Grant Nos. 10135010, 90205025) and INF105-SCE-1-1

** To whom correspondence should be addressed. E-mail: fudx@lnm.imech.ac.cn

upwind difference approximation we have

$$F_j^{(1,+)} = h_{j+1/2}^{(1,+)} - h_{j-1/2}^{(1,+)}, \quad h_{j+1/2}^{(1,+)} = f_j, \quad (3)$$

where the upper index $(k, +)$ (in Eq. (3) $k=1$) denotes that the approximation is kth order accurate for $c>0$. After Taylor series expansion from (3), we have

$$h_{j+1/2}^{(1,+)} - h_{j-1/2}^{(1,+)} = f_j - f_{j-1} = \Delta x\left(\frac{\partial f}{\partial x}\right)_j - \frac{\Delta x}{2}\left[\frac{\partial}{\partial x}\left(\Delta x \frac{\partial f}{\partial x}\right)\right]_j + \cdots, \quad (4)$$

from which we can obtain the second order symmetrical difference approximation using a discretization of the residual term on the right hand side of Eq. (4):

$$F_j^{(2,0)} = h_{j+1/2}^{(2,0)} - h_{j-1/2}^{(2,0)} = h_{j+1/2}^{(1,+)} - h_{j-1/2}^{(1,+)} + \frac{1}{2}\bar{\delta}_x\delta_x^+ f_j + O(\Delta x^3), \quad (5)$$

where

$$h_{j+1/2}^{(2,0)} = h_{j+1/2}^{(1,+)} + \frac{1}{2}\bar{\delta}_x^+ f_j = \frac{1}{2}(f_j + f_{j+1}), \quad (6)$$

$$\delta_x^+ f_j = \mp(f_j \pm f_{j\pm1}), \qquad \delta_x^0 = \frac{1}{2}(\delta_x^+ + \delta_x^-), \quad (7)$$

and the upper index $(k, 0)$ means that the approximation is symmetrical and kth order accurate. From Eq. (4) we can also construct the second order accurate upwind biased difference approximation. For example, for the case $c>0$,

$$F_j^{(2,+)} = h_{j+1/2}^{(2,+)} - h_{j-1/2}^{(2,+)} = h_{j+1/2}^{(1,+)} - h_{j-1/2}^{(1,+)} + \frac{1}{2}\bar{\delta}_x\bar{\delta}_x f_j + O(\Delta x^3),$$

$$h_{j+1/2}^{(2,+)} = h_{j+1/2}^{(1,+)} + \frac{1}{2}\bar{\delta}_x f_j = \frac{1}{2}(3f_j - f_{j-1}). \quad (8)$$

After Taylor series expansion from the second order accurate symmetrical difference approximation, we have

$$F_j^{(2,0)} = \frac{1}{2}(f_{j+1} - f_{j-1}) = \Delta x\left[\frac{\partial f}{\partial x}\right]_j + \frac{\Delta x^2}{3!}\left[\frac{\partial}{\partial x}\left(\Delta x \frac{\partial^2 f}{\partial x^2}\right)\right]_j + O(\Delta x^5),$$

from which we can get the numerical flux with the third order upwind difference approximation:

$$h_{j+1/2}^{(3,+)} = h_{j+1/2}^{(2,0)} - \frac{1}{6}\delta_x^2 f_j = \frac{1}{6}[2f_j + 5f_{j+1} - f_{j-2}], \quad (9)$$

and the fourth order accurate symmetrical difference approximation:

$$h_{j+1/2}^{(4,0)} = h_{j+1/2}^{(2,0)} - \frac{1}{12}[\delta_x^2 f_{j+1} + \delta_x^2 f_j] = \frac{1}{12}[-f_{j+2} + 7(f_{j+1} + f_j) - f_{j-1}]. \quad (10)$$

From the flux residual correction we can construct the higher order accurate approximations. For example, the fifth order upwind difference approximation

$$h_{j+1/2}^{(5,+)} = h_{j+1/2}^{(4,0)} + \frac{1}{30}\delta_x^4 f_j, \quad (11)$$

$$\delta_x^4 f_j = f_{j+2} + f_{j-2} - 4(f_{j+1} + f_{j-1}) + 6f_j,$$

$$h_{j+1/2}^{(5,+)} = \frac{1}{60}[-3f_{j+2} + 27f_{j+1} + 47f_j - 13f_{j-1} + 2f_{j-2}]; \quad (12)$$

the sixth order symmetrical difference approximation

$$h_{j+1/2}^{(6,0)} = h_{j+1/2}^{(4,0)} + \frac{1}{60}(\delta_x^4 f_{j+1} + \delta_x^4 f_j), \quad (13)$$

$$h_{j+1/2}^{(6,0)} = \frac{1}{60}[f_{j+3} + f_{j-2} - 8(f_{j+2} + f_{j-1}) + 37(f_{j+1} + f_j)];$$

the seventh order accurate upwind difference approximation

$$h_{j+1/2}^{(7,+)} = h_{j+1/2}^{(6,0)} - \frac{1}{140}\delta_x^6 f_j, \quad (14)$$

$$\delta_x^6 f_j = f_{j+3} + f_{j-3} - 6(f_{j+2} + f_{j-2}) + 15(f_{j+1} + f_{j-1}) - 20f_j;$$

the eighth order accurate symmetrical difference approximation

$$h_{j+1/2}^{(8,0)} = h_{j+1/2}^{(6,0)} - \frac{1}{280}(\delta_x^6 f_j + \delta_x^6 f_{j+1});$$

the ninth order accurate upwind difference approximation

$$h_{j+1/2}^{(9,+)} = h_{j+1/2}^{(8,0)} + \frac{576}{9!}\delta_x^8 f_j;$$

and the tenth order accurate symmetrical difference approximation

$$h_{j+1/2}^{(10,0)} = h_{j+1/2}^{(8,0)} + \frac{288}{9!}(\delta_x^8 f_j + \delta_x^8 f_{j+1}).$$

In the general case, suppose that at grid points $j-k$, $\cdots, j-1, j, j+1, \cdots, j+k$, we have the $2k$ order accurate symmetrical difference approximation

$$F_j^{(2k,0)} = h_{j+1/2}^{(2k,0)} - h_{j-1/2}^{(2k,0)},$$

from which after Taylor series expansion we can obtain

$$h_{j+1/2}^{(2k,0)} - h_{j-1/2}^{(2k,0)} = \Delta x\left(\frac{\partial f}{\partial x}\right)_j + C\Delta x^{2k+1}\left[\frac{\partial^{2k+1} f}{\partial x^{2k+1}}\right]_j + \cdots = \Delta x\left(\frac{\partial f}{\partial x}\right)_j + C\Delta x^{2k}\left[\frac{\partial^{2k} f}{\partial x^{2k}}\right]_{j+1/2} - C\Delta x^{2k}\left[\frac{\partial^{2k} f}{\partial x^{2k}}\right]_{j-1/2} + O(\Delta x^{2k+2}), \quad (15)$$

where C is a known constant obtained after Taylor series expansion. With grid points $j-k-1, \cdots, j, \cdots, j+k+1$ after discretization of the terms in [ ]

we can get the expression

$$\Delta x^{2k}[\partial^{2k}f/\partial x^{2k}]_{j+1/2}=\frac{1}{2}[\delta_x^{2k}f_{j+1}+\delta_x^{2k}f_j], \tag{16}$$

where

$$\delta_x^{2k}f_j=f_{j-k}-C_{2k}^1f_{j-k+1}+\cdots+(-1)^mC_{2k}^mf_{j-k+m}+\cdots+(-1)^{2k}f_{j+k}. \tag{17}$$

The $2(k+1)$th order accurate symmetrical numerical flux can be written as

$$h_{j+1/2}^{(2k+2,0)}=h_{j+1/2}^{(2k,0)}-\frac{C}{2}[\delta_x^{2k}f_j+\delta_x^{2k}f_{j+1}]. \tag{18}$$

If the approximation $\Delta x^{2k}[\partial^{2k}f/\partial x^{2k}]_{j+1/2}=\delta_x^{2k}f_{j-m}$ is used, the following $(2k+1)$th order accurate upwind biased numerical flux can be obtained:

$$h_{j+1/2}^{(2k+1,+)}=h_{j+1/2}^{(2k,0)}-C\delta_x^{2k}f_{j+m}, \tag{19}$$

where $m\leqslant 0$ for the case $C>0$. The simplest case is $m=0$.

2 Operator extrapolation

In Ref. [12] it is shown that the oscillations are created by the non-uniform group velocity in the numerical solutions. The symmetrical and the weakly upwind biased schemes belong to the class SLOW (denoted as SLW in Ref. [12]), and the strongly upwind biased schemes belong to the class MEXED (denoted as MXD in Ref. [12]). The second Pade scheme belongs to class FAST (denoted as FST in Ref. [12]). To improve the shock resolution it is suggested to use FST/MXD scheme behind the shock, and SLW scheme in front of the shock. Suppose that we have uniformly distributed mesh grid points $j-k, \cdots, j-1, j, j+1, \cdots, j+k$ on which we can construct $2k$ order symmetrical difference approximation for the first derivative, and $(2k-1)$th order upwind biased difference approximation ($m=0$). The correspondingly modified wave numbers are $Ke^{(2k,0)}=Kr^{(2k,0)}+iKi^{(2k,0)}$ and $Ke^{(2k-1,0)}=Kr^{(2k-1,0)}+iKi^{(2k-1,0)}$, where Kr is related with the dissipation of the scheme, and Ki is related with the dispersion. For symmetrical approximation we have $Kr^{(2k,0)}=0$. After eliminating the term $h_{j+1/2}^{(2k,0)}$ from Eqs. (19) and (18), the following relation (for the case of $m=0$) can be obtained

$$h_{j+1/2}^{(2k+1,+)}=h_{j+1/2}^{(2k+2,0)}+\frac{C}{2}[\delta_x^{2k}f_{j+1}-\delta_x^{2k}f_j],$$

from which we can obtain

$$F_j^{(2k+1,+)}=[h_{j+1/2}^{(2k+2,0)}-h_{j-1/2}^{(2k+2,0)}]+\frac{C}{2}[\delta_x^{2k}f_{j+1}-2\delta_x^{2k}f_j+\delta_x^{2k}f_{j-1}]. \tag{20}$$

The term in the first brace of the right hand side of Eq. (20) is related only with the dispersion, and the term in the second brace is related only with the dissipation. From Eq. (20) it can be seen that $Ki^{(2k,0)}=Ki^{(2k-1,0)}$. In this paper, the difference approximation $F_j^{(2k,0)}$ on $j-k, \cdots, j-1, j, j+1, \cdots, j+k$, and $F_j^{(2k+1,+)}$ on $j-k-1, \cdots, j-1, j, j+1, \cdots, j+k$ are used as the original schemes to construct the scheme with the group velocity control. In this case we have $Ki^{(2k+1,+)}>Ki^{(2k,0)}$ or $D^{(2k+1,+)}(Ki)>D^{(2k,0)}(Ki)$ for the most commonly used schemes, where $D(Ki)$ is the group velocity of the numerical solution[12] defined by $\mathrm{d}[K_i(\alpha)]/\mathrm{d}\alpha$. Although we have $D^{(2k+1,+)}(Ki)>D^{(2k,0)}(Ki)$, the scheme $F_j^{(2k+1,+)}$ may not be MXD. To make the scheme MXD, a difference operator extrapolation is introduced.

Consider a linear combination

$$\bar{h}_{j+1/2}^{(2k-1,\pm)}=(1+\sigma)h_{j+1/2}^{(2k-1,\pm)}-\sigma h_{j+1/2}^{(2k,0)}, \tag{21}$$

$$\bar{h}_{j+1/2}^{(2k,\pm)}=(1+\sigma)h_{j+1/2}^{(2k+1,\pm)}-\sigma h_{j+1/2}^{(2k,0)}, \tag{22}$$

where the scheme is symmetrical and SLW for $\sigma=-1$, and it is dissipative for $\sigma>-1$. The scheme with numerical flux (21) has the order of accuracy of $O[(1+\sigma)h^{2k-1}, h^{2k}]$, and the scheme with (22) has the order of accuracy of $O(h^{2k})$. From the above analysis we can see that the linear combination (22) can increase both the dissipation and the group velocity with the increasing parameter $\sigma>-1$, but the linear combination (21) can only increase the dissipation of the scheme with any $\sigma>-1$, and the group velocity of the numerical solutions cannot be changed. In this paper Eq. (22) is used to construct GVC schemes. The linear operator extrapolation (22) leads to enlarged group velocity and the dissipation in the numerical solutions and make the scheme MXD with $\sigma>-1$ without losing the order of accuracy.

3 Improvement of shock resolution with GVC

3.1 Scheme with GVC

Ref. [12] has shown that to improve the shock resolution it is suggested to use SLW scheme in front of the shock, and FST/MXD scheme behind the shock. Fig. 1 and Fig. 2 give the variations of the

group velocity $D(Ki)/D\alpha$ and Kr as a function $\alpha = k\Delta x$ for the case of $k=2$ (fourth order accurate) in scheme with (22), and Fig. 3 and Fig. 4 show the variations of $D(Ki)/D\alpha$ and Kr for the case of $k=3$ (sixth order accurate).

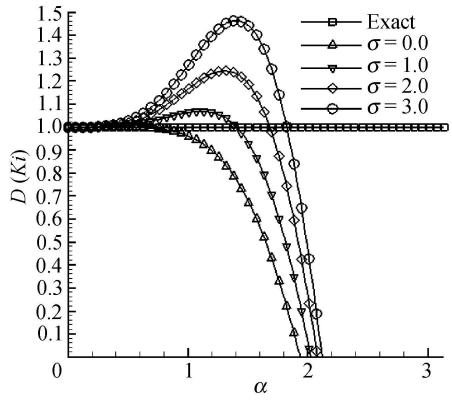

Fig. 1. Variation of $D(Ki)/D\alpha$ versus α ($k=2$).

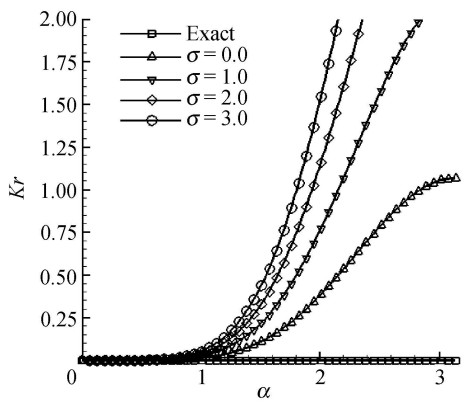

Fig. 2. Variation of Kr versus α ($k=2$).

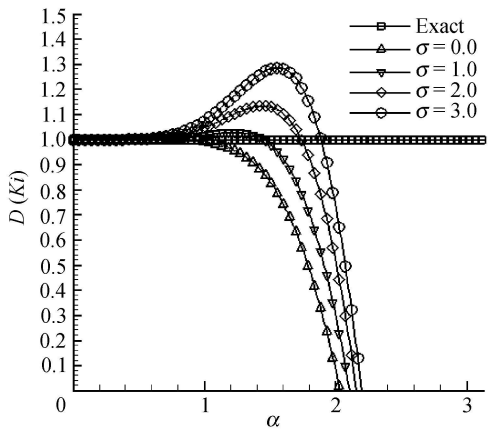

Fig. 3. Variation of $D(Ki)/D(\alpha)$ versus α ($k=3$).

It can be seen from Figs. 1—4 that the scheme is dissipative ($\sigma > -1$) and MXD for large σ. The numerical flux of the $2k$th order schemes after modification with GVC is expressed as

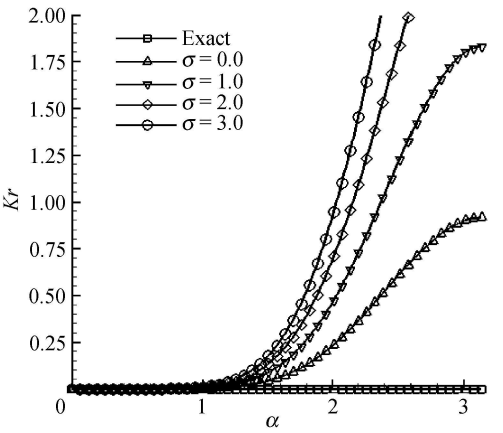

Fig. 4. Variation of Kr versus α ($k=3$).

$$F_j^{(2k)} = H_{j+1/2}^{(2k)} - H_{j-1/2}^{(2k)},$$
$$H_{j+1/2}^{(2k)} = H_{j+1/2}^{(2k,+)} + H_{j+1/2}^{(2k,-)},$$
$$H_{j+1/2}^{(2k,\pm)} = \frac{1 \pm SS(j+1/2)}{2} h_{j+1/2}^{(2k,\pm)} + \frac{1 \mp SS(j+1/2)}{2} h_{j+1/2}^{(2k,0)}, \quad (23)$$

where $h_{j+1/2}^{(2k,\pm)}$ is obtained from (22) and the corresponding scheme is MXD after operator extrapolation. In computation, the SS function is expressed as[12]

$$SS(f_{j+1/2}) = \frac{1}{2}[SS(f_{j+1}) + SS(f_j)], \quad (24)$$
$$SS(f_j) = \mathrm{sign}(\delta_x^0 f_j \cdot \delta_x^2 f_j). \quad (25)$$

For the aerodynamics equations the density ρ or the pressure p can be used as the function f in (25). Expression (23) makes the scheme MXD behind the shock and SLW in front of the shock, and therefore the GVC requirement is satisfied for improvement of the shock resolution.

3.2 Weighted group velocity control (WGVC)

The above presented NFRC + GVC method is still difficult to solve the discontinuity with high pressure ratio for the high order scheme (higher than second order accuracy: $k > 1$). In this section the so-called WGVC method is introduced. Practical application shows that good resolution of the shock can be obtained with the following modified GVC scheme

$$H_{j+1/2}^{(2k,\pm)} = \frac{1 \pm SS(j+1/2)}{2} h_{j+1/2}^{(2k,\pm)} + \frac{1 \mp SS(j+1/2)}{2} h_{j+1/2}^{(2k,0)}, \quad (26)$$
$$h_{j+1/2}^{(2k,\pm)} = (1 - g_{j+1/2}^{(2k)}) h_{j+1/2}^{(2k,\pm)} + g_{j+1/2}^{(2k)} h_{j+1/2}^{(2,\pm)},$$
$$h_{j+1/2}^{(2k,0)} = (1 - g_{j+1/2}^{(2k)}) h_{j+1/2}^{(2k,0)} + g_{j+1/2}^{(2k)} h_{j+1/2}^{(2,0)}, \quad (27)$$

$$g_{j+1/2}^{(2k)} = [\sigma_{0,j+1/2}]^{2k}. \quad (28)$$

The function $\sigma_{0,j+1/2}$ is defined in our computation as

$$\sigma_{0,j+1/2} = \frac{|\delta_x^+ f_j|}{\max_j |\delta_x^+ f_j| + \varepsilon}, \quad (29)$$

$$\sigma_{0,j+1/2} = \frac{|f_{j+1} - f_j|}{|f_{j+1}| + |f_j| + \varepsilon}, \quad (30)$$

where $\varepsilon \approx 10^{-5}$ is a small parameter. From the definition (28, 29) it can be seen that $g_{j+1/2}^{(2k)} \approx [O(\sigma_0 \Delta x)]^{2k}$ and the constructed scheme has $2k$ order accuracy in the smooth region. With large parameter σ in Eq. (22) we can enlarge the wave interval where the scheme has FST property and increase the dissipation in the uncontrollable wave interval without losing the order of accuracy. $\sigma = 3$ is used in our computation. The process of scheme construction is as follows: 1) construct the high order accurate NFRC schemes; 2) make the upwind biased scheme MXD with operator extrapolation; 3) modify the scheme with weighting; 4) control the group velocity of numerical solution for having shock with high resolution.

4 Numerical experiments

The above presented method was used to solve practical problems, for example, the propagation of the linear shock, the steady state shock tube problem, the Sod model problem, the 2-D Riemman problem, and the shock-material surface interaction problem. From the view point of inviscid flow, the thickness of the shock is zero, the derivative does not exist at the shock, and therefore the high order accurate scheme does not help much for shock capturing. Our purpose of constructing the high order accurate scheme is to simulate the complex flow field with the N-S equations. The numerical examples are given in this section just to show the capability of shock capturing with the developed schemes. Eq. (30) is used in computation.

4.1 1-D steady state shock tube problem

The one-dimensional Euler equations are discretized with both the fourth and sixth order accurate NFRC+WGVC schemes for the cases of $M_\infty = 2$, 5, and 10. Fig. 5 shows the pressure distribution for the case of $M_\infty = 10$ with the fourth order accurate NFRC+WGVC, and Fig. 6 presents the pressure distribution for the sixth order accurate NFRC + WGVC scheme.

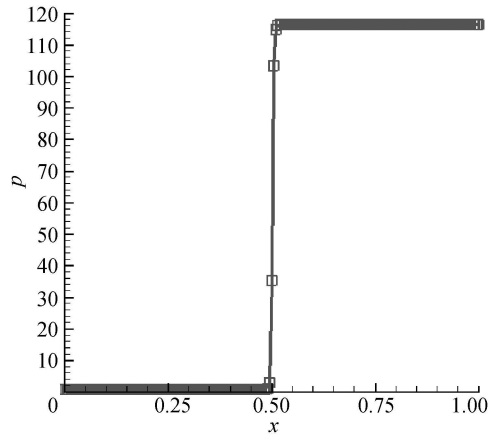

Fig. 5. Pressure with the 4th order NFRC+WGVC.

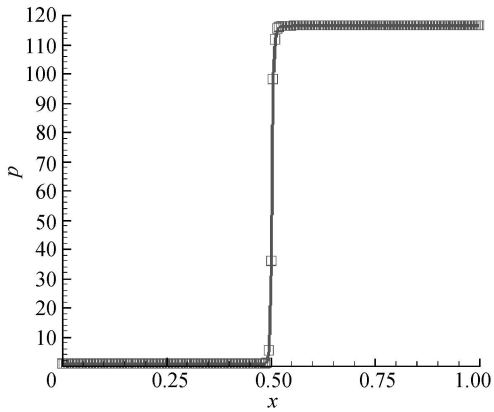

Fig. 6. Pressure with the 6th order NFRC+WGVC.

4.2 1-D Sod model problem[13]

The distributions of the fluid parameters at the beginning $t = 0$ are as follows

$$p = 1, \quad \rho = 1, \quad u = 0;$$
$$p = 0.1, \quad \rho = 0.125, \quad u = 0.$$

Figs. 7 and 8 give the pressure and density distributions with the 4th order accurate NFRC+WGVC at $t = 0.14$. Figs. 9 and 10 show the pressure and density distributions with the 6th order accurate NFRC + WGVC. The exact solutions are also given for comparison.

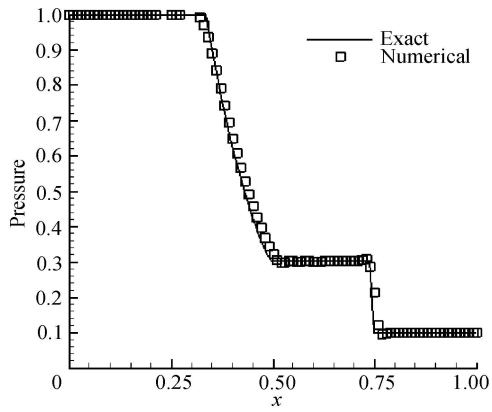

Fig. 7. Pressure with the 4th order NFRC+WGVC.

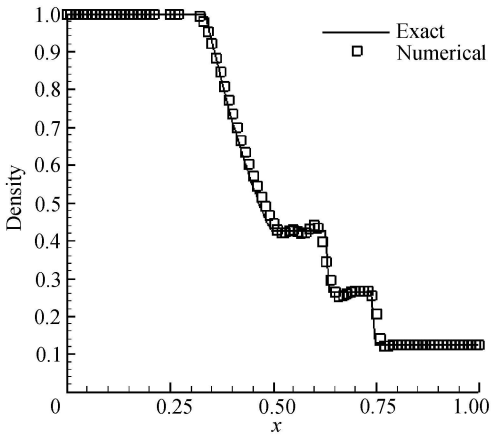

Fig. 8. Density with the 4th order NFRC+WGVC.

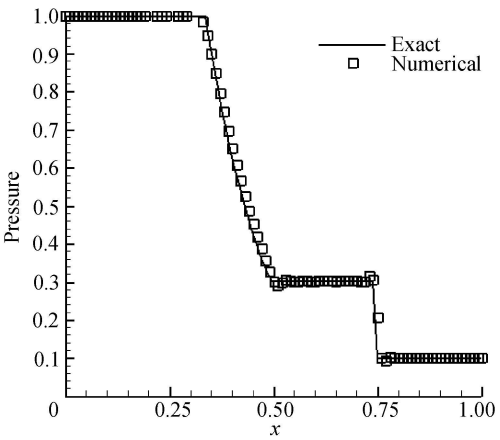

Fig. 9. Pressure with the 6th order NFRC+WGVC.

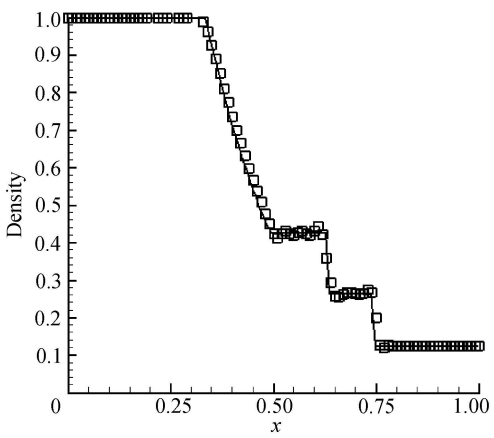

Fig. 10. Density with the 6th order NFRC+WGVC.

4.3 1-D Shu-Osher shock tube problem

The initial data are given as follows:

$$\rho = 3.857,\ u = 2.629,\ p = 10.33,\quad \text{for } 0 \leqslant x < 0.1,$$

$$\rho = 1 + a\sin(\varpi x),\ u = 0.0,\ p = 1.0,\quad \text{for } 0.1 \leqslant x \leqslant 1.0.$$

In computation $a=0.3$ and $\varpi=40$ are used. Fig. 11 gives the result with the fourth order accurate NFRC+GVC at $t=0.2$ with number of mesh grid points $N=401$. Fig. 11 also gives a result with number of grid points $N=5001$ which is considered to be the exact solution. The agreement is quite well. Fig. 12 presents the result with the 6th order NFRC+GVC with the same mesh grid points. In computation the parameter $\sigma_{0,j+\frac{1}{2}} = 0$ (without weighting) in Eq. (29) is used.

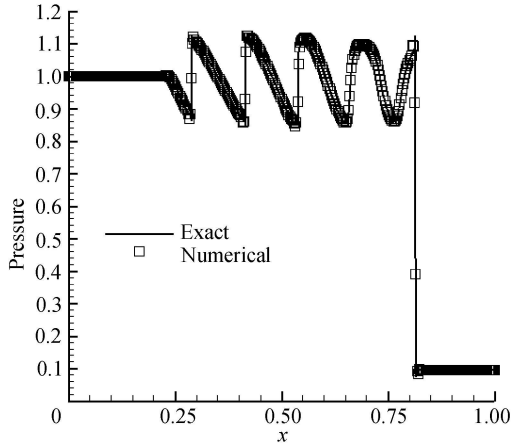

Fig. 11. Pressure with the 4th order NFRC+GVC at $t=0.2$.

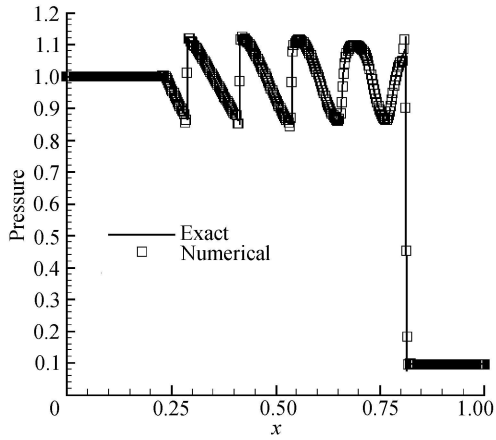

Fig. 12. Pressure with the 6th order NFRC+GVC at $t=0.2$.

4.4 2-D Riemman problem[13]

The initial distribution of the physical parameters is as follows:

$\rho_1=1.5,\quad p_1=1.5,\quad u_1=0.0,\quad v_1=0.0;$

$\rho_2=0.5323,\quad p_2=0.3,\quad u_2=1.206,\quad v_2=0.0;$

$\rho_3=0.1379,\quad p_3=0.029,\quad u_3=1.206,\quad v_3=1.206;$

$\rho_4=0.5323,\quad p_4=0.3,\quad u_4=0.0,\quad v_4=1.206;$

The index k of the fluid parameter g_k shows that g_k is distributed in the subdomain with index k (Fig. 13). This problem was computed with the 4th order and 6th order NFRC+WGVC. The density contours

computed with the 6th order NFRC+WGVC at $t=0.6$ are given in Fig. 14, and the pressure contours are given in Fig. 15.

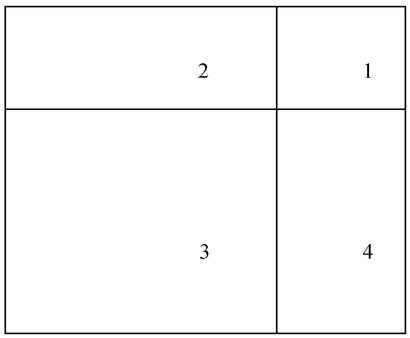

Fig. 13. Schematic diagram for distribution of fluid parameters at $t=0$.

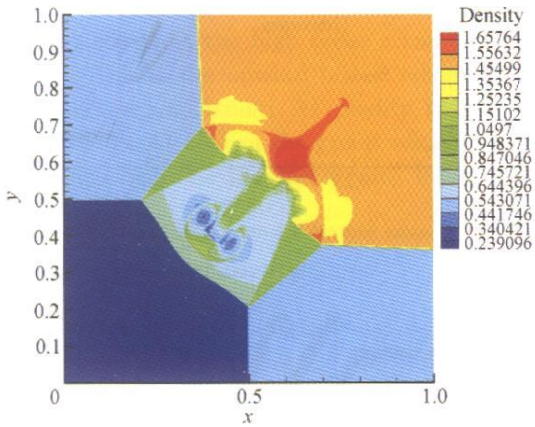

Fig. 14. Density contours of 2-D Riemman problem at $t=0.6$.

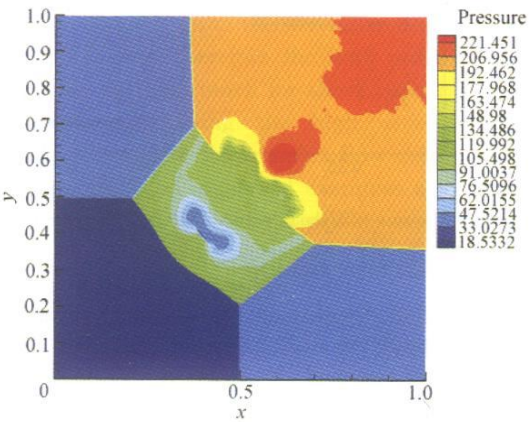

Fig. 15. Pressure contours of Riemman problem at $t=0.6$.

4.5 Numerical simulation of R-M instability problem

The R-M instability is the instability of accelerated material interface driven by moving shock between two different media. The R-M instability has attracted attention of many researchers recently because of the importance of this kind of problems in inertial confinement fusion (ICF) and explosion of supernova. As an example, this problem is solved with the scheme developed in this paper. The sixth order accurate WGVC method is used to approximate the convection terms of the two-dimensional compressible N-S equations in cylindrical coordinate, and the viscous terms of the N-S equations are approximated with the traditional sixth order accurate difference approximation.

At $t=0$ we have a shock as shown in Fig. 16 (a). The shock is moving toward to the center with shock Mach number $Ms=1.2$. The Reynolds number is $Re=50000$ based on the radius of the averaged material interface at $t=0.0$. The light gas is inside the interface. The initial conditions are given in Ref. [14]. The moving shock will interact with the material interface. Some results are shown in Fig. 16, from which we see the development of R-M instability. After shock-interface interaction, the reflected rarefaction wave goes outward, and the transmitted shock goes toward the center. After multiple interaction of the waves between the material interface and the center we obtain the typical spike-bubble structure (Fig. 16(c)). We can see the phase changing clearly from Fig. 16(a)—(c). Fig. 16(d) gives the wave structure showing the interaction between the transmitted shocks at the time $t=0.39$.

5 Summary

(i) A new method of high order accurate difference approximation with NFRC is presented. The method is simple, and the scheme with any order of accuracy can be obtained easily.

(ii) A simple linear operator extrapolation is introduced to control the dissipation and dispersion of the scheme.

(iii) The constructed NFRC scheme is modified with group velocity control (GVC) and weighted group velocity control (WGVC) to improve the resolution of the shock.

(iv) The constructed NFRC+GVC (or NFRC+WGVC) scheme is used to solve physical problems, and the obtained results are satisfactory.

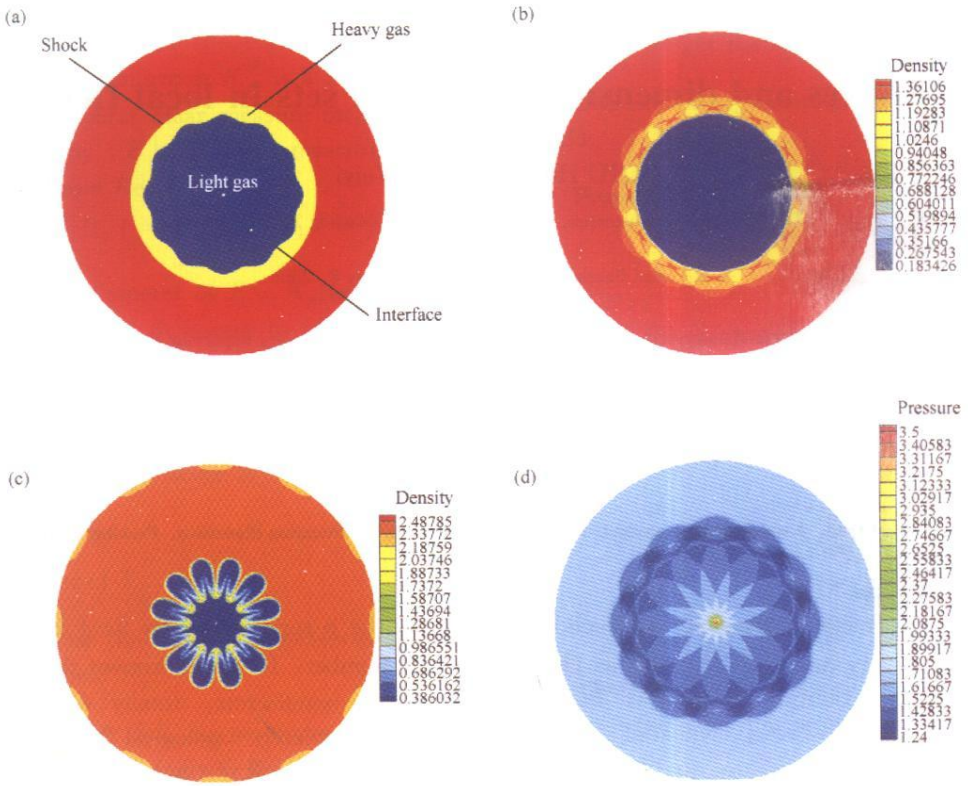

Fig. 16. Computed results at different times: (a) Density contours at $t=0.00$; (b) density contours at $t=0.30$; (c) density contours at $t=3.3$; (d) pressure contours at $t=0.39$.

References

1 Ma Y.W., Gao H., Fu D.X. et al. Difference scheme on non-uniform mesh and their application. Progress in Natural Science, 2004, 14(10): 848—854.

2 Peyret R. Introduction to high-order approximation methods for computational fluid dynamics. In: Advanced Flow Computations, New York: Springer, 2000, 1—80.

3 Fu D.X. and Ma Y.W. Numerical simulation of physical problems and high order accurate schemes. J. Comput. Phys. (in Chinese), 1992, 9(4): 501—505.

4 Lerat A. and Corre C. A Residual-based compact scheme for the compressible Navier-Stokes equations. J. Compt. Phys., 2001, 170: 642—675.

5 Corre C., Hanss G. and Goncalves E. Accurate computation of laminar boundary-layer flows using a residual-based scheme. In: Proceedings of BAIL2002, An International Boundary and Interior Layers Computational & Asymptotic Methods, Western Australia 8th—12th July, 2002.

6 Yee H.C., Warming R.F. and Harten A. Implicit total variation diminishing (TVD) schemes for steady state calculations. AIAA 83—1902, 1983.

7 Harten A., Engquist B., Osher S. et al. Uniformly high order accurate essentially non-oscillatory schemes III. J. Comput. Phys., 1987, 71: 231—303.

8 Liu X.D. and Osher S. Convex ENO high order multi-dimensional schemes without field by field decomposition or staggered grids. J. Comput. Phys., 1998, 142: 302—338.

9 Shu C.W. Essentially non-oscillatory and weighted essencially non-oscillatory schemes for hyperbolic conservation laws. NASA/CR-97-206253, ICASE Report No. 97—65.

10 Liu R.X. and Shu C.W. Some New Methods in Computational Fluid Dynamics. Beijing: Science Press, 2003.

11 Balsara D.S. and Shu C.W. Monotonicity preserving weighted essentially non-oscillatory schemes with increasingly high-order accuracy. J. Comput. Physics, 2001, 160: 405—452.

12 Fu D.X. and Ma Y.W. A high order accurate difference scheme for complex flow fields. J. Compt. Phys., 1997, 134: 1—15.

13 Sod G.A. A survey of several finite difference methods for system of non-linear hyperbolic conservation laws. J. Comput. Phys., 1978, 27(1): 1—32.

14 Fu D.X. and Ma Y.W. Numerical simulation of Richtmyer-Meshkov instability. Science in China (Series A), 2004, 4(Supplement): 234—244.